

Optical properties of well-defined granular metal systems

T. Yamaguchi, M. Sakai, and N. Saito

Research Institute of Electronics, Shizuoka University, Johoku, Hamamatsu 432, Japan

(Received 21 November, 1984)

Optical properties of granular metal systems prepared by alternate vacuum deposition of Ag and MgF₂ have been studied. Mean thickness of Ag island films and MgF₂ spacer layers were about 0.2 and 5 nm, respectively. Three samples consisting of 1, 10, and 50 island films were prepared, which are denoted as S_1 , S_{10} , and S_{50} , respectively. Optical properties of S_1 were well explained by the simple formula for the two-dimensional (2D) system. Those of S_{50} were well explained by the Bruggeman theory (BT) for the 3D system rather than by the Maxwell-Garnett theory (MGT). Those of S_{10} could not be explained by BT as well as by MGT, because the thickness of the sample is so small that the influence of the sample surface cannot be ignored. In each case the dielectric constants contributed by bound electrons in silver fine particles were found to be modified from those of the bulk, which suggests also a modification of the energy-band structure.

I. INTRODUCTION

It is important to understand the optical properties of granular metal systems because of their application to solar absorbers.¹⁻⁴ It is also important to know the electronic structure of a fine metal particle because catalytic action of fine metal particles depends on their size⁵⁻¹⁰ and because the activity of sensors is enhanced by the use of fine metal particles.¹¹ The electronic structure in fine metal particles has been studied optically,¹²⁻¹⁵ by electron spectroscopy for chemical analysis [x-ray photoemission spectroscopy (XPS) or ultraviolet photoemission spectroscopy],¹⁶⁻²⁰ and by the extended x-ray absorption method.²¹

Two basic theories have already been proposed for the optical properties of the three-dimensional (3D) granular metal system, the Maxwell-Garnett theory²² (MGT) and the Bruggeman theory^{23,24} (BT). Abeles and Gittleman^{2,3} have shown that the MGT explained their experiments better than the BT. Their conclusion is based on the fact that plasma resonance absorption has appeared in a sample with $Q \approx 0.4$, where Q is the volume fraction of metal, and the BT does not predict the appearance of the plasma resonance absorption for a sample with $Q > \frac{1}{3}$ whereas MGT predicts it for any value of Q .

Here we shall show that this is not always the case. The particle size of their sample was more than 10 nm and was not very much smaller than the sample thickness of 64 nm (Ref. 1). Thus the BT does not seem to be applicable to such a case. Generally, theories for the 3D granular metal system assume infinite extent of the sample. If the thickness of a sample is small compared with the particle size, the optical behavior will reflect only the effect near the sample surface rather than the volume effect. To verify the theory for the 3D granular metal system experimentally, we should take samples with small metal fractions as well as thicker samples. Then the volume effect becomes dominant, and coagulation between particles and irregularity in particle shape will be minimized.

Although MGT and BT give exactly the same absorption curve for small Q , e.g., $Q < 10^{-3}$, the theories already differ sufficiently at $Q = 0.05$.²⁵ So we have prepared samples with $Q \approx 0.05$.

Since the effective dielectric constant of a granular metal system, ϵ , is a function of those of the metal particles, ϵ_m , and of the dielectric matrix, ϵ_d , we need to know the latter for the calculation of ϵ . Sample preparation by cosputtering or coevaporation, as done by Cohen *et al.*,¹ may obscure the exact value of ϵ_d , because the matrix may contain metal atoms.

We extensively studied optical properties of two-dimensional (2D) granular metal systems, i.e., island films, and clarified the geometrical structure as well as the size dependence of ϵ_m in island particles.^{14,15} Based on these results, we have constructed 3D granular metal systems by depositing alternately metal island films and dielectric matrix layers. Optical constants of the evaporated MgF₂ matrix layer have been measured in advance.

II. EXPERIMENT

Ag and MgF₂ were deposited alternately on a fused-quartz substrate in an ordinary vacuum chamber of 10^{-4} -Pa range. Mean incident thickness monitored by a quartz oscillator was about 0.4 nm for the silver island film and about 5 nm for the MgF₂ spacer layer, the latter being nearly equal to the interisland spacing. The layer numbers of the silver island films were 10 and 50, these samples being denoted as S_{10} and S_{50} , respectively. Transmittance of the sample was measured by a dual-beam spectrophotometer (Nihon Bunkou Co., UVIDEC-505) with a bare substrate as a reference.

Optical properties of the single island film, which is denoted as S_1 , were measured by multiple attenuated total-reflection spectroscopy (ATR). Details of the ATR method are given in our earlier papers.^{14,15} A hundred repetitions of total reflections enhanced the sensitivity for small optical absorption of the submonolayer metal film

which was deposited on a fused-quartz ATR prism in an ultrahigh vacuum chamber in the 10^{-6} -Pa range.

III. THEORIES AND ANALYTICAL METHODS

A. Single island film

Optical absorption of a metal island film is given as a function of the following complex quantity:²⁶

$$\alpha = 1/[F + 1/(\epsilon_m - 1)], \quad (1)$$

where F , the effective depolarizing factor of the island particles, is a real number between 0 and 1. ϵ_m is the complex dielectric constant of a metal particle, which consists of two terms,

$$\epsilon_m = \epsilon_f + \delta\epsilon_b, \quad (2)$$

where ϵ_f is the Drude term contributed by the free electrons,

$$\epsilon_f = 1 - \omega_p^2/(\omega^2 - i\omega\omega_\tau) \quad (3)$$

and $\delta\epsilon_b$ is the contribution of the bound electrons. The classical size effect requires ω_τ to be given by

$$\omega_\tau = v_F/r, \quad (4)$$

where v_F is the Fermi velocity of free electrons and r the radius of the spherical particle.

At present there are no theories explaining the size effect on the $\delta\epsilon_b$ contributed by the bound electrons. We have found that $\delta\epsilon_b$ of fine island particles of Ag (Ref. 14) and Au (Ref. 15) should be modified from that of the bulk. In this paper we make a better modification of $\delta\epsilon_b$.

B. Modification of $\delta\epsilon_b$

We modify $\delta\epsilon_b$ as follows: firstly we replace the joint density of states (JDOS) near the onset of the interband transition by the following empirical functions:

$$J = J_0 + (J_h - J_0)\{1 - \exp[-A\hbar(\omega - \omega_0)]\} \quad \text{for } \omega > \omega_0, \quad (5)$$

$$J = J_0 \exp[-(J_h/J_0 - 1)A\hbar(\omega_0 - \omega)] \quad \text{for } \omega < \omega_0,$$

i.e., two exponential functions are smoothly combined at (ω_0, J_0) , where the slope is determined by A . The tails of the exponential functions tend to zero and J_h for negative and positive directions, respectively, as shown in Fig. 1(a). We use the bulk value when J exceeds it in the higher-energy region. Using the modified J we obtain the imaginary part of $\delta\epsilon_b$ from the relation $J = \delta\epsilon_b''(\hbar\omega)^2$. The real part is given using the Kramers-Kronig relations as shown in Fig. 1(b).

C. Single MgF₂ layer

The following empirical formula approximated from the Drude-Lorentz theory was applied to the evaporated MgF₂ layer:

$$n^2[\text{Re}(\epsilon_d)] = B + C\lambda^2/(\lambda^2 - \lambda_0^2), \quad (6)$$

$$k = \lambda^3/[n(\lambda^2 - \lambda_0^2)^2].$$

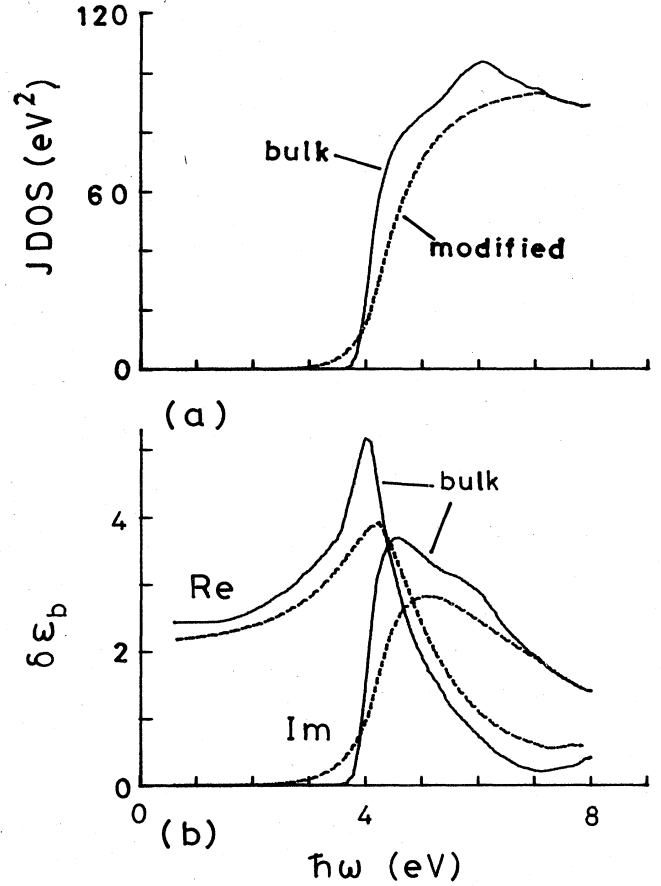


FIG. 1. (a) JDOS [$=\delta\epsilon_b''(\hbar\omega)^2$] and (b) $\delta\epsilon_b$ of silver island particles. Solid lines show the bulk value. Dashed lines show the best modification from the bulk.

D. Maxwell-Garnett theory

The Maxwell-Garnett theory gives the formula²²

$$\frac{\epsilon - \epsilon_d}{\epsilon + 2\epsilon_d} = Q \frac{\epsilon_m - \epsilon_d}{\epsilon_m + 2\epsilon_d}, \quad (7)$$

where ϵ , ϵ_d , and ϵ_m are the dielectric constants of the system, the dielectric matrix, and the metal particles, respectively. Q is the packing density of the particles, i.e., volume fraction of the metal. Equation (7) can be rewritten as

$$\epsilon = \epsilon_d + Q \frac{\epsilon_d}{(1-Q)/3 + \epsilon_d/(\epsilon_m - \epsilon_d)}. \quad (8)$$

E. Bruggeman theory

The Bruggeman theory gives the formula^{23,24}

$$Q \frac{\epsilon_m - \epsilon}{\epsilon_m + 2\epsilon} + (1-Q) \frac{\epsilon_d - \epsilon}{\epsilon_d + 2\epsilon} = 0, \quad (9)$$

where notations are the same as Eq. (7). This can be rewritten as

$$4\epsilon = \epsilon_d + (3Q - 1)(\epsilon_m - \epsilon_d) \pm \{ [(3Q - 1)(\epsilon_m - \epsilon_d) + \epsilon_d]^2 + 8\epsilon_m \epsilon_d \}^{1/2}. \quad (10)$$

F. Curve-fitting analysis

The imaginary part of α multiplied by d_w is obtained from the ATR experiments, where d_w is the mean thickness or weight thickness of the metal deposit. For the single MgF_2 layer as well as for S_{10} and S_{50} , transmittance of the sample was calculated by the usual formula for a plane-parallel film with total thickness d .

Observed spectra were analyzed by the curve-fitting method. Common fitting parameters for granular metal systems were $\hbar\omega_\tau$ and those for the modification of J in Eq. (5), i.e., J_0 , J_h , $\hbar\omega_0$, and A . $\hbar\omega_p$ was fixed at the bulk value of 9.15 eV. Other fitting parameters are F and d_w for Eq. (1), and Q and d for Eqs. (8) and (10). Fitting parameters for the single MgF_2 layer are B , C , and λ_0 in Eq. (6) as well as the thickness d .

IV. RESULTS

A. Single island film (S_1)

Dashed lines in Fig. 2 show the normalized α'' measured by the ATR method. Solid lines are the best-fit curves with (a) the bulk $\delta\epsilon_b$ and (b) $\delta\epsilon_b$ modified from the bulk as shown in Fig. 1. Solid lines in Fig. 1 show (a) JDOS and (b) $\delta\epsilon_b$ of the bulk silver, and dashed lines show the modified curves. The best fit values of param-

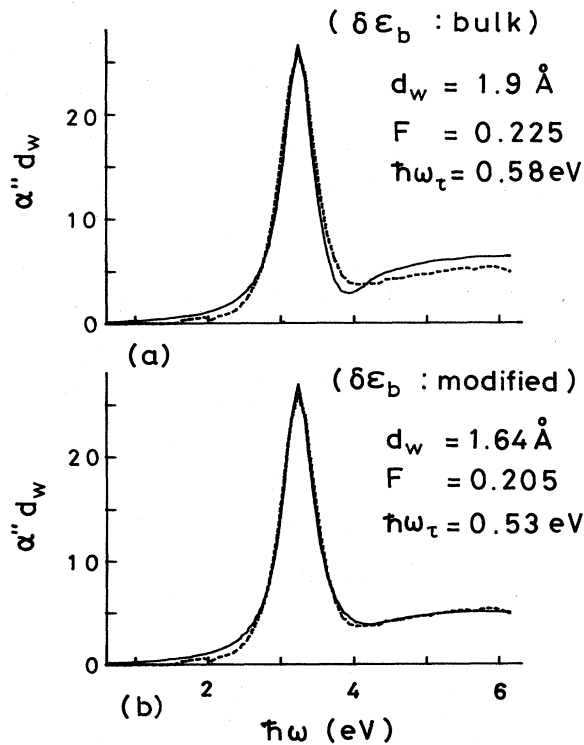


FIG. 2. Normalized α'' of a silver island film (S_1). Dashed lines show the measured values. Solid lines show the best-fit curves using (a) the bulk $\delta\epsilon_b$ and (b) the modified $\delta\epsilon_b$.

eters in Eq. (5) are $\hbar\omega_0 = 4.2$ eV, $J_0 = 30$ eV², $J_h = 95$ eV², and $A = 1.3$ eV⁻¹.

As we see in Fig. 2(b), the measured and the calculated curves agree sufficiently well with each other. The best-fit values of the parameters are given in the figure. $\hbar\omega_\tau \approx 0.5$ eV corresponds to a particle size of about 4 nm, which is consistent with the electron micrograph.¹⁴ Since the best-fit value of d_w was 0.164 nm, the packing density Q of silver in S_{10} and S_{50} must be around 0.04.

B. Single MgF_2 layer

Dashed lines in Fig. 3(a) show the measured transmittance and reflectance spectra of a single MgF_2 layer deposited on a fused-quartz substrate with the same condition of deposition as for S_{10} and S_{50} . Solid lines show those calculated using the best-fit parameters, i.e., $B = 1.7$, $C = 0.2$, and $\lambda_0 = 170$ nm in Eq. (6) and $d = 207$ nm. Solid lines in Figs. 3(b) and 3(c) show the calculated

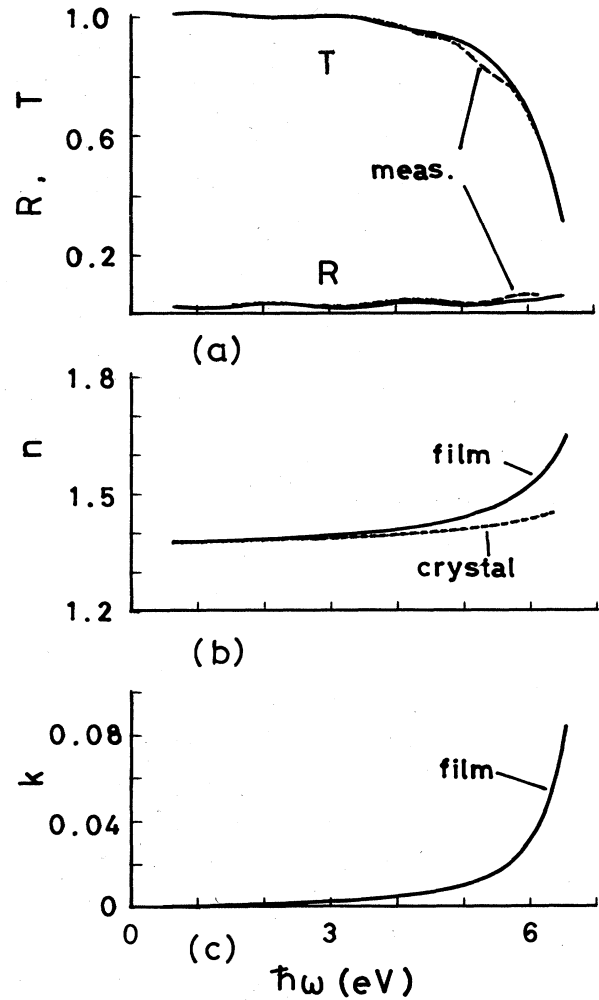


FIG. 3. (a) Transmittance T and reflectance R , (b) refractive index n , and (c) extinction coefficient k of an evaporated MgF_2 film 207-nm thick. Solid lines show calculated curves. Dashed lines in (a) show the measured T and R . The dashed line in (b) shows n of the crystal MgF_2 .

n and k of the MgF_2 layer, respectively. The dashed line in Fig. 3(b) shows n of the crystal MgF_2 .²⁷

C. S_{50}

Dashed lines in Fig. 4 show the measured transmittance spectra of S_{50} . Solid lines show the best-fit curves using the bulk $\delta\epsilon_b$ [Figs. 4(a) and 4(b)] and the modified $\delta\epsilon_b$ [Figs. 4(c) and 4(d)] by MGT [Figs. 4(a) and 4(c)] or by BT [Figs. 4(b) and 4(d)]. The best-fit values of the parameters are given in each figure.

D. S_{10}

Dashed lines in Fig. 5 show the measured transmittance spectra of S_{10} . Solid lines in Figs. 5(a) and 5(b) show the calculated curves using the same parameters as in Figs. 4(c) and 4(d), respectively, except the total thickness d is replaced by

$$d = (205 \text{ nm})(10+1)/(50+1) \simeq 44 \text{ nm}.$$

As the calculated curves are so different from the measured one, the optical properties of S_{10} must be quite different from those of S_{50} . Thus we change the parameters, Q , $\hbar\omega_\tau$, and d , by the following process.

First change Q to match the position of the plasma resonance absorption, i.e., from 0.035 to 0.3 in MGT and from 0.035 to 0.1 in BT. Next change d to match the height in the higher photon energy region. Finally change $\hbar\omega_\tau$ to match the height of the plasma resonance absorption.

Solid lines in Figs. 5(c)–5(f) show the calculated curves. In Figs. 5(c) and 5(d) we stress the matching around the plasma resonance absorption, while in Figs. 5(e) and 5(f) the matching in the whole spectral range.

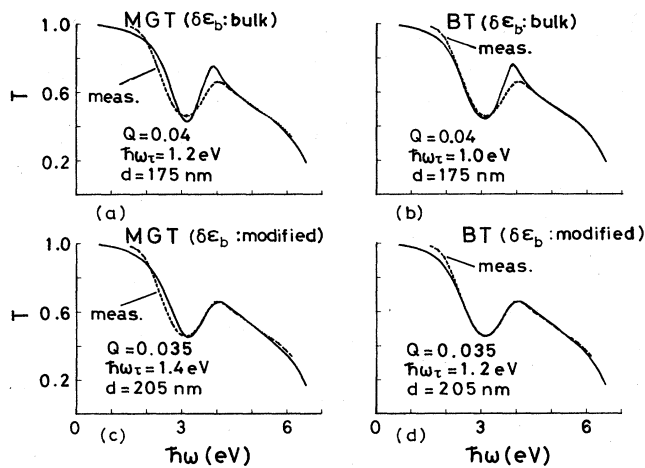


FIG. 4. Transmittance T of S_{50} . Dashed lines show the measured values. Solid lines show the best-fit curves using the bulk $\delta\epsilon_b$ [(a) and (b)] and the modified $\delta\epsilon_b$ [(c) and (d)] by MGT [(a) and (c)] or by BT [(b) and (d)]. The best-fit values of the parameters are given in each figure.

V. DISCUSSION

We can see in Fig. 4(d) that the two curves agree quite well with each other. We need no complicated assumptions such as a log-normal distribution in particle size or a fictitious plasma frequency of electrons as in the work of Granqvist and Hunderi.⁴ Essential are the appropriate modification of $\delta\epsilon_b$, the effect of the sample thickness and the exact values of n and k of the MgF_2 dielectric matrix. These factors were not taken into consideration sufficiently in earlier works.^{1–4}

Comparing Fig. 4 and Fig. 5, we see the importance of the sample thickness. The best agreement between two curves is realized by MGT rather than BT for S_{10} as shown in Fig. 5(e) though it is still insufficient. Since the imaginary parts of Eqs. (1) and (8) have similar forms, the optical behavior of S_{10} should look like that of the single island film. The sample of Gittleman and Abeles,^{1–3} which required MGT rather than BT, is equivalent to S_{10} rather than S_{50} . As the best-fit values of d and Q in Fig. 5 are so different from the expected values, it is concluded that the optical behavior of S_{10} cannot be explained by BT or by MGT. Island particles in S_{10} are located less than five island layers from the sample surface, whereas 80% of the island particles in S_{50} are located more than five island layers from the sample surface. Therefore a new theory taking account of the influence of sample sur-

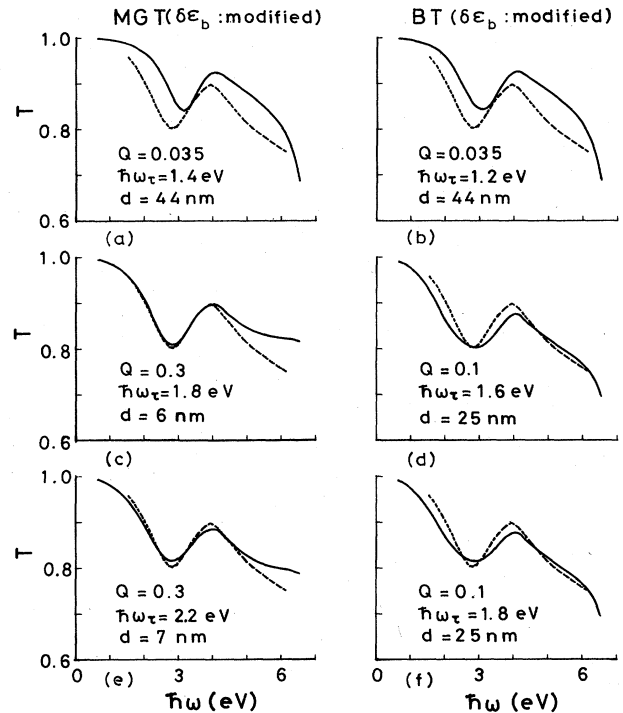


FIG. 5. Transmittance T of S_{10} . Dashed lines show the measured curves. Solid lines in (a) and (b) show curves calculated using the same parameters as in Figs. 4(c) and 4(d), respectively. Solid lines in (c)–(f) show curves calculated varying the three parameters in order to match them to the measured curves. (c) and (d) stress the matching in the spectral range around the plasma resonance absorption, while (e) and (f) the matching in the whole spectral range.

face will be necessary for the interpretation of S_{10} .

As seen in Figs. 2(b) and 4(d), the observed spectra are almost reproduced by the use of the commonly modified $\delta\epsilon_b$. In previous papers^{14,15} we have shown the following. (a) The smaller the particles are, the larger the modification is. (b) The modification is consistent with the XPS studies on fine metal particles.¹⁶⁻²⁰ (c) Optical absorption of an island film composed of particles larger than 10 nm is well explained by Eq. (1) with the bulk $\delta\epsilon_b$.

We have also shown¹⁴ that the modification of $\delta\epsilon_b$ in metal particles cannot be explained by the modification of the energy-band structure due to lattice contraction.²⁸ Particles in S_{50} are surrounded by the solid MgF_2 ; thus lattice contraction due to surface tension must be small compared with that of the island particles in vacuum. Since the modified $\delta\epsilon_b$ is the same for particles in vacuum as well as in the solid MgF_2 , the modification seems essential for a small metal system without lattice contraction, though a recent paper²⁹ explained a shift of reflectance peak, observed around $\hbar\omega \simeq 22$ eV with an Au island film, by the lattice contraction.

Next we discuss the importance of the exact values of n and k of the dielectric matrix. We tried to fit curves calculated using constant values of n and $k=0$, which is often assumed in earlier works, or using the table value of crystal MgF_2 shown by a dashed line in Fig. 3(b). However, it was difficult to get reasonable matching between measured and calculated curves. Therefore the exact values of n and k of the dielectric matrix were found to be necessary for the analysis.

Although the best fit value of $\hbar\omega_r = 0.53$ eV in Fig. 2(b) is consistent with a particle size of about 4 nm,¹⁴ it became 1.2 eV in Fig. 4(d), which is too large. The idea of lattice defects within small particles^{30,31} cannot solve the problem because particles are the same for the two cases.

We have shown that the same problem of a too large value of $\hbar\omega_r$ exists in the case of island films composed of large island particles, or thicker films, though the influence of the irregularity in particle shape was taken into account.¹⁵ We have shown in an earlier paper³² that the retarded dipole-dipole interactions in thick island films cause the damping of the plasma resonance, i.e., if we do not take the retarded dipole-dipole interactions into account, the value of $\hbar\omega_r$ becomes too large. Granqvist and Hunderi⁴ calculated the retardation effects in BT but they concluded that the effect is small for small Q , e.g., $Q < 0.1$.

This problem may be solved by a new theory,³³ which claims that the irregular position of metal particles causes the damping. However we have not performed the analysis with the new theory, because the shape of the plasma resonance absorption predicted by it is too asymmetric.

VI. CONCLUSIONS

Optical properties of 3D-granular metal systems can be explained by BT rather than by MGT in agreement with the recent paper.³⁴ The modification of $\delta\epsilon_b$ from the bulk value, the sample thickness and exact values of n and k of the dielectric matrix are found to be essential for the explanation of the optical properties of 3D granular metal systems. We will be able to get information about the energy-band structure in fine metal particles from the empirical function of JDOS.

ACKNOWLEDGMENT

We wish to thank Professor A. Ichikawa of Shizuoka University for a critical reading of the manuscript.

-
- ¹R. W. Cohen, G. D. Cody, M. D. Coutts, and B. Abeles, *Phys. Rev. B* **8**, 3689 (1973).
- ²B. Abeles and J. I. Gittleman, *Appl. Opt.* **15**, 2328 (1976).
- ³J. I. Gittleman and B. Abeles, *Phys. Rev. B* **15**, 3273 (1977).
- ⁴C. G. Granqvist and O. Hunderi, *Phys. Rev. B* **16**, 1353 (1977); **18**, 1554 (1978); *J. Appl. Phys.* **50**, 1058 (1979).
- ⁵M. Boudart, *Adv. Catal.* **20**, 153 (1969).
- ⁶D. W. McKee, *J. Phys. Chem.* **67**, 841 (1963).
- ⁷J. R. Carter, J. A. Cuusumano, and J. H. Sinfelt, *J. Phys. Chem.* **70**, 2257 (1966).
- ⁸R. L. Burwell, Jr. and J. B. Cohen, *J. Catal.* **53**, 414 (1978).
- ⁹J. F. Hamilton, *J. Vac. Sci. Technol.* **13**, 319 (1976).
- ¹⁰J. F. Hamilton and R. C. Baetzold, *Science* **205**, 1213 (1979).
- ¹¹S.-C. Chang, *J. Vac. Sci. Technol. A* **1**, 296 (1983).
- ¹²U. Kreibig, *J. Phys. (Paris) Colloq.* **38**, C2-97 (1977).
- ¹³U. Kreibig, in *Growth and Properties of Metal Clusters*, edited by J. Bourdon (Elsevier, Amsterdam, 1980), p. 371.
- ¹⁴T. Yamaguchi, M. Ogawa, H. Takahashi, N. Saito, and E. Anno, *Surf. Sci.* **129**, 232 (1983).
- ¹⁵T. Yamaguchi, M. Takiguchi, S. Fujioka, H. Takahashi, and E. Anno, *Surf. Sci.* **138**, 449 (1984).
- ¹⁶M. G. Mason and R. C. Baetzold, *J. Chem. Phys.* **64**, 271 (1976).
- ¹⁷K. S. Liang, W. R. Salaneck, and I. A. Aksay, *Solid State Commun.* **19**, 329 (1976).
- ¹⁸M. G. Mason, L. J. Gerenser, and S.-T. Lee, *Phys. Rev. Lett.* **39**, 288 (1977).
- ¹⁹H. Roulet, J.-M. Mariot, G. Dufour, and C. F. Hougue, *J. Phys. F* **10**, 1025 (1980).
- ²⁰G. Apai, S.-T. Lee, and M. G. Mason, *Solid State Commun.* **37**, 213 (1981).
- ²¹G. Apai, J. F. Hamilton, J. Stohr, and A. Thompson, *Phys. Rev. Lett.* **43**, 165 (1979).
- ²²J. C. Maxwell-Garnett, *Philos. Trans. R. Soc. London* **203**, 385 (1904).
- ²³D. A. G. Bruggeman, *Ann. Phys. (Leipzig)* **24**, 636 (1935).
- ²⁴D. Stroud, *Phys. Rev. B* **12**, 3368 (1975).
- ²⁵T. Yamaguchi, *J. Vac. Soc. Jpn.* **27**, 809 (1984), in Japanese.
- ²⁶ $[2\epsilon_s/(1+\epsilon_s)]\alpha$ is the effective polarizability of an island particle on a substrate surface, where the factor in [] arose from mirror-image effect. ϵ_s is the dielectric constant of the substrate (Refs. 14 and 26). 4π does not appear because we have calculated with mksa units.
- ²⁷*AIP Handbook*, 3rd ed., edited by Dwight E. Gray (McGraw-Hill, New York, 1972), pp. 6-35.
- ²⁸S. A. Nepijko, E. Pippel, and J. Woltersdorf, *Phys. Status*

- Solids A **61**, 469 (1980).
- ²⁹P. Picozzi, S. Santucci, M. De Crescenzi, F. Antonangeli, and M. Piacentini, Phys. Rev. B **31**, 4023 (1985).
- ³⁰U. Kreibig, Z. Phys. B **31**, 39 (1978).
- ³¹E. Anno and R. Hoshino, J. Phys. Soc. Jpn. **50**, 1209 (1981).
- ³²T. Yamaguchi, S. Yoshida, and A. Kinbara, J. Opt. Soc. Am. **64**, 1563 (1974).
- ³³B. N. J. Persson and A. Liebsch, Solid State Commun. **44**, 1637 (1982); Phys. Rev. B **28**, 4247 (1983); **29**, 6907 (1984).
- ³⁴K. D. Cummings, J. C. Garland, and D. B. Tanner, Phys. Rev. B **30**, 4170 (1984).